atmosphere

MDPI

Article

$PM_{2.5}$-Related Health Risk during Chinese Spring Festival in Taizhou, Zhejiang: The Health Impacts of COVID-19 Lockdown

Quanquan Wu [1], Xianglian Wang [2], Kai Ji [3], Haibing Qiu [3], Weiwei Feng [1], Shan Huang [1,*], Ting Huang [1], Jianlong Li [1] and Daishe Wu [1]

[1] Key Laboratory of Poyang Lake Environment and Resource Utilization, Ministry of Education, School of Resources and Environment, Nanchang University, Nanchang 330031, China
[2] School of Civil and Architectural Engineering, Nanchang Institute of Technology, Nanchang 330099, China
[3] Xinjiang Rao River Hydrological and Water Resources Monitoring Center, Shangrao 334001, China
* Correspondence: coral119@ncu.edu.cn

Abstract: Exposure to high concentrations of fine particles ($PM_{2.5}$) with toxic metals can have significant health effects, especially during the Chinese spring festival (CSF), due to the large amount of fireworks' emissions. Few studies have focused on the potential health impact of $PM_{2.5}$ pollution in small cities in China during the 2020 CSF, which coincided with the COVID-19 outbreak that posed a huge challenge to the environment and obvious health issues to countries around the world. We examined the characteristics of $PM_{2.5}$, including carbonaceous matter and elements, for three intervals during the 2020 CSF in Taizhou, identified the sources and evaluated the health risks, and compared them with those of 2018. The results showed that $PM_{2.5}$ increased by 13.20% during the 2020 CSF compared to those in the 2018 CSF, while carbonaceous matter (CM) and elements decreased by 39.41% and 53.84%, respectively. The synergistic effects of emissions, chemistry, and transport may lead to increased $PM_{2.5}$ pollution, while the lockdown measures contributed to the decrease in CM and elements during the 2020 CSF. Fe, Mn, and Cu were the most abundant elements in $PM_{2.5}$ in both years, and As and Cr(VI) should be of concern as their concentrations in both years exceeded the NAAQS guideline values. Industry, combustion, and mineral/road dust sources were identified by PCA in both years, with a 5.87% reduction in the contribution from industry in 2020 compared to 2018. The noncarcinogenic risk posed by As, Co, Mn, and Ti in 2018 and As and Mn in 2020 was significant. The carcinogenic risk posed by As, Cr(VI), and Pb exceeded the accepted precautionary limit (1×10^{-6}) in both years. Mn was the dominant contributor to the total noncarcinogenic risks, while Cr(VI) showed the largest excessive cancer risks posed by metals in $PM_{2.5}$, implying its associated source, industry, was the greatest risk to people in Taizhou after exposure to $PM_{2.5}$. Despite the increase in $PM_{2.5}$ mass concentration, the health impacts were reduced by the lockdown policy implemented in Taizhou during the 2020 CSF compared to 2018. Our study highlights the urgent need to consider the mitigation of emissions in Taizhou and regional joint management efforts based on health protection objectives despite the rough source apportionment by PCA.

Keywords: $PM_{2.5}$; health risk; COVID-19; trace metals; Chinese spring festival

check for updates

Citation: Wu, Q.; Wang, X.; Ji, K.; Qiu, H.; Feng, W.; Huang, S.; Huang, T.; Li, J.; Wu, D. $PM_{2.5}$-Related Health Risk during Chinese Spring Festival in Taizhou, Zhejiang: The Health Impacts of COVID-19 Lockdown. *Atmosphere* **2022**, *13*, 2099. https://doi.org/10.3390/atmos13122099

Academic Editor: Francesca Costabile

Received: 9 November 2022
Accepted: 12 December 2022
Published: 14 December 2022

Publisher's Note: MDPI stays neutral with regard to jurisdictional claims in published maps and institutional affiliations.

Copyright: © 2022 by the authors. Licensee MDPI, Basel, Switzerland. This article is an open access article distributed under the terms and conditions of the Creative Commons Attribution (CC BY) license (https://creativecommons.org/licenses/by/4.0/).

1. Introduction

The public health risks associated with exposure to fine particles (fine PM with a 50% cut-off aerodynamic diameter of 2.5 μm ($PM_{2.5}$)) and air pollution have attracted increasing attention from the public, governments, and health organizations around the world [1]. $PM_{2.5}$ is considered to be a major contributor to haze, causing not only reduced visibility but also health hazards [2,3]. Recent studies have shown that $PM_{2.5}$ reduces life expectancy because of health effects on morbidity and mortality [4], particularly for lung cancer [5] and cardiovascular disease [6]. The population-weighted average of $PM_{2.5}$ annual concentrations in China during 2013 was 61 $\mu g/m^3$ [7], not reaching the WHO

interim target level 1 (35 μg/m^3). Therefore, the health effects caused by $PM_{2.5}$ exposure have become an urgent issue in China.

Because of its large specific surface area, $PM_{2.5}$ has been found to have the ability to attach various pollutants, including heavy metals and organic compounds, potentially increasing its mutagenic and carcinogenic risks [8]. Accumulated evidence suggests that transition metals in $PM_{2.5}$ are strongly associated with oxidative DNA damage, although their mass is low compared to other components [9]. In order to assess the toxicity of metals associated with $PM_{2.5}$, many studies have been conducted on the concentrations and spatial and temporal variabilities of different metals embedded in $PM_{2.5}$, relying on long-term monitoring activities or short-term sampling events [3,10–12]. Traffic, residential energy use, industry, power plants, dust, and waste combustion are the main sources of $PM_{2.5}$ [13–15]. Fireworks burning is also considered to be a significant source of air pollution, as fireworks are used to celebrate festivals and events around the world [3]. The particles and gases emitted from fireworks deteriorate air quality and increase the risk to human health [16–22].

A novel coronavirus (COVID-19) was reported in Wuhan in December 2019, which quickly expanded across China since the outbreak was coincident with the human migration of the Chinese spring festival (CSF) [23]. A national lockdown measure was imposed, reducing transportation, economic, and social activities; social distancing measures were also tightened by other countries [24–26]. This provided an opportunity to evaluate the sources of $PM_{2.5}$ and potential health impacts during the CSF.

Many studies have reported significant improvements in air quality during city lockdowns (CLDs) [27–30]. In contrast, haze pollution still occurs because of unfavorable meteorological conditions [31–33] and long-range transport [34,35]. Currently, a large number of studies have been conducted in major cities where fireworks are banned, and few studies have focused on $PM_{2.5}$ pollution and the resulting potential health impacts in small cities in China with a "limited fireworks" policy using systematic observations from both conventional and COVID-19 outbreak years. Since $PM_{2.5}$ and its associated metals vary in concentrations across geographic regions, the diversity of findings requires field consideration in small cities rather than the direct adoption of relevant management strategies derived from the major city studies described above.

We aimed to assess the changes in ambient $PM_{2.5}$ and the health risks of $PM_{2.5}$-bound metals during the implementation of the lockdown measures in Taizhou, a small city in China in Zhejiang province, after the COVID-19 outbreak in 2020. We collected samples before and after the lockdown during the 2020 CSF and compared them with those from the same period in 2018. The differences in the sources of carbonaceous matter and heavy metals in $PM_{2.5}$ between 2018 and 2020 were identified. Based on the concentrations of heavy metals in $PM_{2.5}$, the health risks of human exposure to heavy metals in $PM_{2.5}$ through inhalation were evaluated. We hope this study will enable the recommendation of targeted environmental policies in Taizhou.

2. Materials and Methods

2.1. Study Area and Sampling

Taizhou is located in the middle of the East China Sea coast of Zhejiang province, with a population of 6.6 million and an area of 9411 km^2. The sampling site (28.5994 N, 121.0954 E) is located in a rural area in the south-central part of the city, with no factories nearby (Figure 1). There is no fireworks ban here.

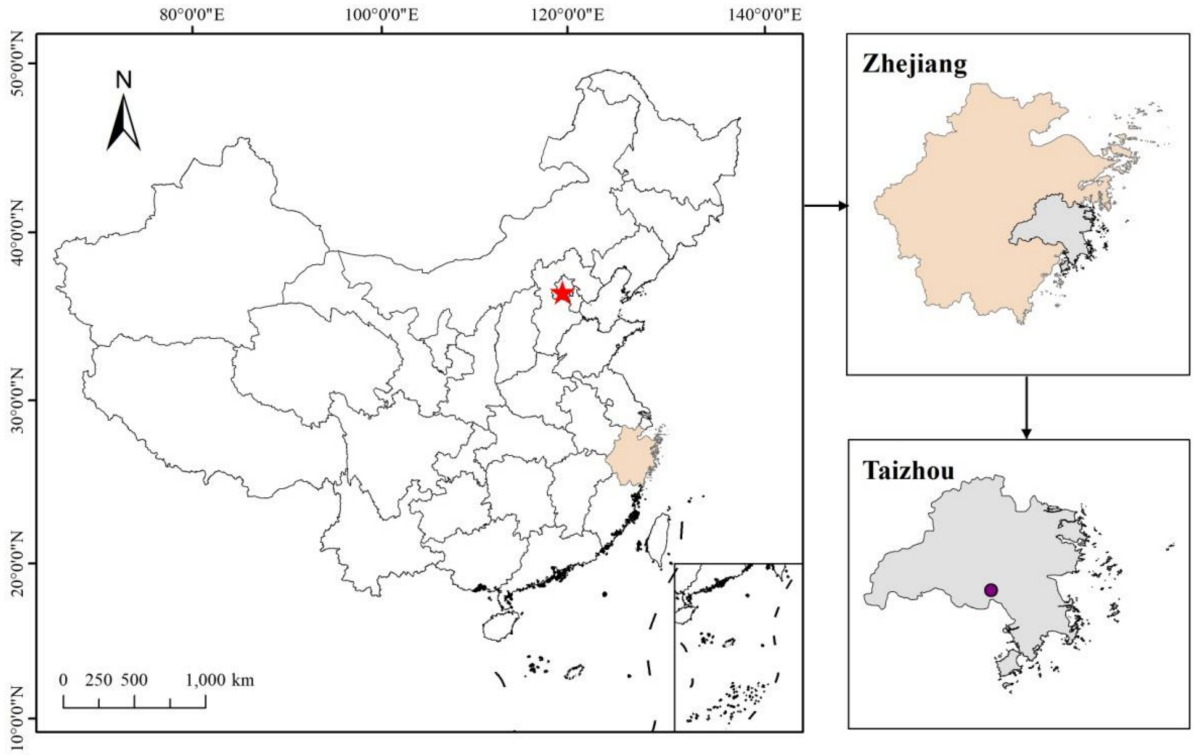

Figure 1. Sampling site in this study.

The sampling campaigns were conducted during CSF in 2018 and 2020. Sampling activities took place from 5 to 20 February 2018 and from 18 January to 12 February 2020, with 23 h of sampling per day. A portable particle sampler (Mini-vol TAS-5.0; Airmetrics, Springfield, OR, USA) was deployed on the roof of a two-story building to collect $PM_{2.5}$ with quartz filters (Whatman; 47 mm, CAT No.1851-047) from the air at a flow rate of 5 L/min. The pump flow rate was corrected to 5 ± 0.05 L/min before and after sampling using a soap film flow calibrator (Gilibrator-2; Sensidyne, St. Petersburg, FL, USA).

Prior to sampling, the quartz filters were pre-cleaned at 500 °C for 6 h to remove volatile impurities and equilibrated in a desiccator at 25 °C and 40% relative humidity for 48 h. The filters were weighed on an analytical balance (AR224CN; Ohaus, Parsippany, NJ, USA) before and after sampling. The $PM_{2.5}$ samples were stored in sealed polyethylene bags at −20 °C until further analysis.

The Lunar New Year in 2018 and 2020 fell on 16 February 2018 and 25 January 2020, respectively. As shown in Table 1, the sampling period was divided into three sections according to the human activities: (1) 5–14 February 2018 (10 days) and 16–23 January 2020 (8 days), before SF (pre-SF), when people prepared for the holiday and national lockdown on 23 January 2020; (2) 15–20 February 2018(6 days) and 24–30 January 2020 (7 days), the CSF holiday (SF), including Lunar New Year's Eve (big fireworks evening, 24 January) and Lunar New Year's day (CSF, 25 January 2020); and (3) 31 January–11 February 2020 (12 days), when people stayed at home because of lockdown measures (post-SF).

Table 1. Time period description in 2018 CSF and 2020 CSF.

Sampling Period	Pre-SF	SF	Post-SF	Lunar New Year
2018 CSF	5–14 February 2018	15–20 February 2018	/	16 February 2018
2020 CSF	16–23 January 2020	24–30 January 2020	31 January−11 February 2020	25 January 2020

2.2. Chemical Analysis

Half of each filter sample was cut into pieces and placed in a digestion tube containing 20 mL of HCl-HNO_3 digestion solution. The digestion was carried out at 100 °C for 2 h using an electric oven digester (BHW-09C heating block; BOTONYC, Shanghai, China). After cooling to room temperature, the digests were filtered through a 0.22 m filter and then diluted to 50 mL with deionized water. Ten elements (As, Ba, Co, Cr, Cu, Fe, Mn, Pb, Sr, and Ti) were analyzed using inductively coupled plasma optical emission spectroscopy (ICP-OES, iCAP 7000; Thermo Fisher, Waltham, MA, USA). The method detection limits (MDLs) from the OES instrument were in the range of 0.001–0.03 $\mu g/m^3$. The recoveries of all elements were in the range of 95–105%.

A 0.495 cm^2 punch from the sample filter was used to analyze the organic carbon (OC) and elemental carbon (EC) in $PM_{2.5}$ samples by a thermal/optical carbon analyzer (DRI 2015; Atmoslytic, Calabasas, CA, USA) following the IMPROVE_A protocol. The analyzer was calibrated daily with a known quantity of CH_4. MDLs for OC and EC were 0.18 $\mu gC/cm^2$ and 0.04 $\mu gC/cm^2$, respectively. One sample was analyzed in duplicate from each group of 10 samples. The difference between OC and EC determined from the duplicate analyses was less than 10%.

2.3. Human Exposure and Health Risk Assessment Model

The health risk assessment model recommended by USEPA was adopted in this paper (EPA, 2011). The risk effects consisted of noncarcinogenic and carcinogenic risk assessments according to USEPA IRIA and IARC. In this study, we mainly calculated the health risks caused by respiratory intake.

Inhalation exposure concentrations (ECi, $\mu g/m^3$) of a given TMs were calculated as follows [36]:

$$EC_i = \frac{C_i \times ET \times EF \times ED}{AT} \quad (1)$$

where C_i is the exposure concentration of metals in $PM_{2.5}$ ($\mu g/m^3$); ET is the exposure time (24 h/day); EF is the exposure frequency (180 days/year); ED is the exposure duration (24 years for adults); and AT is the averaging time (for noncarcinogens, AT = ED × 365 days × 24 h/day, and for carcinogens, AT = 70 years × 365 days/year × 24 h).

The hazard quotient (HQ) for noncarcinogenic effects and carcinogenic risks (CRs) from exposure to the selected $PM_{2.5}$-bound TMs were calculated as follows:

$$HQ = EC_i/(RfC_i \times 1000\ \mu g/mg) \quad (2)$$

$$CR = IUR_i \times EC_i \quad (3)$$

where RfC_i is the reference concentration for inhalation exposure for a given metal (mg/m^3); and IUR_i is the inhalation unit risk ($(\mu g/m^3)^{-1}$). An HQ value below 1 is ascribed no significant risk of non-cancer health effects, whereas a value above 1 indicates a chance at which noncarcinogenic effects may occur [37]. Furthermore, as for the carcinogenic risk, the acceptable precautionary criterion is from 1×10^{-6} to 1×10^{-4} [37]. For regulatory purposes, a CR value of 1×10^{-6} is adopted as the precautionary criterion in the present study [38].

The RfC_i, IUR_i, and standard default values for exposure parameters were taken from the user's guide and technical background document of the US Environmental Protection Agency (EPA) regional screening level (RSL) summary table (TR =1×10^{-6}, HQ = 1) [39]. The hazard index (HI), equal to the sum of HQ, is used to assess the overall potential for noncarcinogenic effects:

$$HI = \sum HQ \quad (4)$$

In this study, since Cr was not speciated into Cr(III) and Cr(VI) and only the total Cr concentration was measured in each fraction, the CR of Cr (VI) was calculated as one-seventh of the total Cr concentration, based on the fact that the concentration ratio of Cr(VI)

to Cr(III) in the air is about 1:6 [40]. We did not discuss Fe, Cu, Zn, and Ti because their RfC_i values were unavailable.

3. Results and Discussion

3.1. Impact of COVID-19 on the Characteristics of $PM_{2.5}$ during the CSF

Figure 2 shows the mass variations of $PM_{2.5}$ over the same sampling period in 2018 and 2020. The mean concentrations of $PM_{2.5}$ were 112.77 ± 49.45 μg/m^3 and 127.66 ± 29.48 μg/m^3 during the observation period in 2018 and 2020, respectively, which reached three–four times the annual value (35 μg/m^3) recommended in the National Ambient Air Quality Standard of China (NAAQS, GB3095-2012). Compared to 2018, Taizhou experienced an increase in $PM_{2.5}$ in 2020, although some studies showed that quarantine measures led to an improvement in air quality [29,30,41]. Our results are consistent with studies in Beijing-Tianjin-Hebei (BTH) and Shanghai, which point to unfavorable meteorological conditions contributing to this outcome [33,34]. Low temperatures and high relative humidity (RH) during the wintertime usually favor the formation of sulfate, nitrate, and ammonium (SNA) aerosols. NO_2 is a major contributor to atmospheric soot and haze, and atmospheric oxidants can promote the formation of secondary particles [42]. Therefore, we looked into the meteorological conditions (temperature, relative humidity, and wind speed) and NO_2 and O_3 levels from the website of the Ministry of Ecology and Environmental of the People's Republic of China and found that the similar meteorological condition, the sudden drop in NO_2 (Table S1 (Supplementary Materials)), and the slightly elevated O_3 level after the COVID-19 outbreak do not explain the observed increased $PM_{2.5}$ pollution in CSF-2020 well. Thus, the synergistic effects of emissions, chemistry, and transport may have led to increased $PM_{2.5}$ pollution during CSF-20 [34,43,44]. Both the mean and median $PM_{2.5}$ concentrations showed a downward trend throughout the study period in 2020, which could be attributed to the reduction in vehicles and industry activities following the national lockdown [12,45].

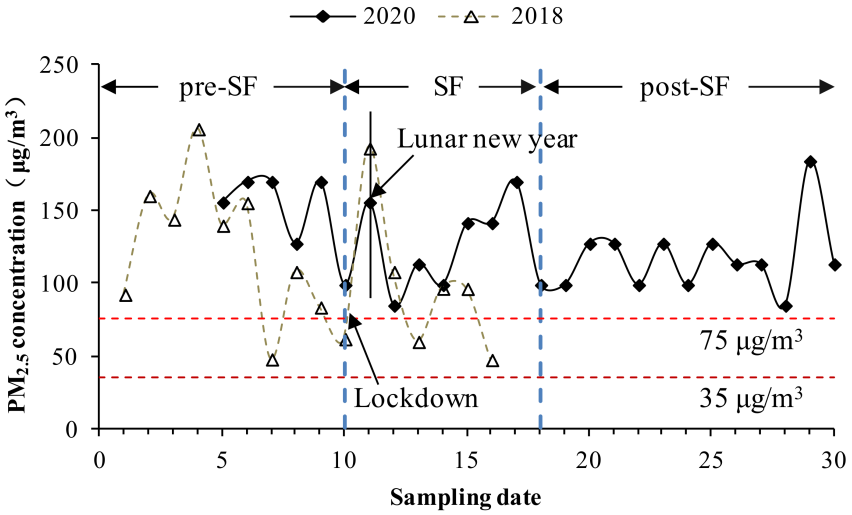

Figure 2. $PM_{2.5}$ mass concentration during CSF in 2018 and 2020.

The average $PM_{2.5}$ concentrations reached 120.17 μg/m^3 and 148.94 μg/m^3 in the pre-SF-2018 and pre-SF-2020, respectively; reduced to 100.44 μg/m^3 and 125.30 μg/m^3 in the SF-2018 and SF-2020, with a reduction of 16.42% and 15.87%, respectively; then, rose back up to 116.75 μg/m^3 in post-SF-2020. This temporal pattern is consistent with the typical fluctuation of energy demand before, during, and after the CSF holidays, as discussed in Shanghai [34]. The intensive fireworks displays and cross-region transport of humans and vehicles, caused by the return of migrant workers to their hometowns, contributed to the high $PM_{2.5}$ level in the pre-SF period [46,47]. $PM_{2.5}$ peaks in 2018 and 2020 were observed in all three intervals owing to fireworks/firecrackers burning during

festivals (Lunar New Year's day, the Lantern festival) and rituals, which were also found in Shanghai, Chengdu, and Xiamen [47–49].

Concentrations of carbonaceous matter and trace elements in $PM_{2.5}$ are summarized in Table 2. During 2018 CSF, the concentrations of OC and EC were 30.743 ± 2.416 μg/m^3 and 6.063 ± 1.834 μg/m^3 in the pre-SF period and 28.527 ± 2.416 μg/m^3 and 4.767 ± 1.827 μg/m^3 in the SF period, respectively. The mean OC/EC ratios were 5.293 and 6.906 in pre-SF and SF periods in 2018, respectively. The OC/EC ratio over three intervals during 2020 CSF was higher than that in 2018. After the lockdown, the mean OC/EC values increased first and then decreased, highlighting a decrease in the relative contribution of primary emissions to carbonaceous pollutants during the SF period [50], as EC is derived from the incomplete combustion of residential coal, vehicle fuels, and biomass and an increase in the relative contribution of secondary emissions during the post-SF period in 2020.

Table 2. Carbonaceous and trace elements in $PM_{2.5}$ in different intervals (μg/m^3).

2018	Pre-SF	SF	2020	Pre-SF	SF	Post-SF
OC	30.743 ± 3.656	28.527 ± 2.416	OC	28.897 ± 6.436	15.113 ± 1.787	15.372 ± 3.815
EC	6.063 ± 1.834	4.767 ± 1.827	EC	4.019 ± 1.337	1.612 ± 0.466	3.074 ± 2.241
OC/EC	5.293 ± 0.978	6.906 ± 3.036	OC/EC	7.962 ± 3.190	9.832 ± 1.989	6.544 ± 3.373
CM	55.252 ± 7.165	6.906 ± 3.036	CM	50.255 ± 10.146	25.792 ± 3.284	27.669 ± 7.534
As	0.084 ± 0.018	0.084 ± 0.021	As	0.070 ± 0.020	0.030 ± 0.024	0.036 ± 0.026
Ba	-	-	Ba	0.152 ± 0.011	0.262 ± 0.234	0.158 ± 0.022
Cd	-	-	Cd	0.005 ± 0.001	0.003 ± 0.003	0.003 ± 0.001
Co	0.014 ± 0.000	0.019 ± 0.001	Co	-	-	-
Cr	0.128 ± 0.022	0.157 ± 0.013	Cr	0.009 ± 0.001	0.010 ± 0.001	0.010 ± 0.001
Cu	0.355 ± 0.073	0.398 ± 0.060	Cu	0.199 ± 0.017	0.242 ± 0.030	0.215 ± 0.030
Fe	5.052 ± 3.625	3.625 ± 0.616	Fe	1.489 ± 0.166	1.555 ± 0.203	1.465 ± 0.142
Mn	0.506 ± 0.093	0.299 ± 0.161	Mn	0.419 ± 0.032	0.542 ± 0.119	0.442 ± 0.047
Pb	0.176 ± 0.068	0.313 ± 0.120	Pb	0.087 ± 0.018	0.069 ± 0.020	0.043 ± 0.016
Ti	0.154 ± 0.052	0.227 ± 0.028	Ti	0.034 ± 0.003	0.034 ± 0.003	0.031 ± 0.004

Carbonaceous matter (CM), which is the sum of organic matter (OM = 1.6 OC (Turpin and Lim, 2001)) and EC, was 55.25 μg/m^3 in pre-SF, reduced by 8.76% to 50.41 μg/m^3 during SF-2018. Since EC only comes from primary combustion emissions and behaves inertly to chemical reactions, the ratio of CM to $PM_{2.5}$ can somewhat reflect the relative changes between secondary production and primary emission [51]. As shown in Figure 3, CM accounted for 17.50–78.59% of $PM_{2.5}$, with an average value of 38.12%. The highest CM value occurred on 9 February 2018 (Little New Year, a week before the Lunar New Year).

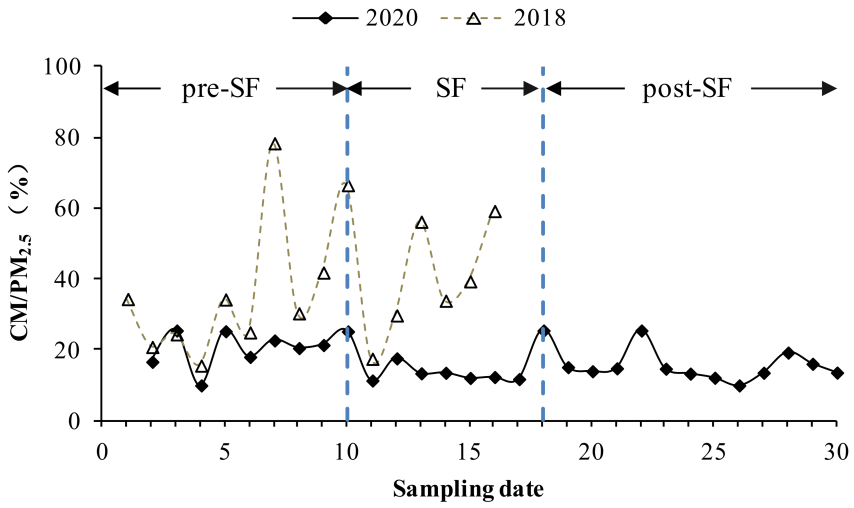

Figure 3. CM/$PM_{2.5}$ during CSF in 2018 and 2020.

In the 2020 observation period, CM values were 43.72–70.57 μg/m^3, accounting for 10.09–25.61% of $PM_{2.5}$, with an average value of 16.76%. The CM in the pre-SF period was similar to the level in 2018 at 50.25 μg/m^3 but was significantly reduced by 48.68% to 25.79 μg/m^3 in the SF period. A decrease in CM/$PM_{2.5}$ occurred during SF and COVID lockdown, followed by an increase during the post-COVID period. This result indicates that secondary aerosol production was enhanced relative to primary emissions during SF and COVID lockdown compared to the pre- and post-COVID phases. Similar cases were observed in other cities [12,52].

The concentrations of 10 trace elements are presented in Table 2. The $PM_{2.5}$-bound metal concentrations in 2020 were lower than those in 2018, despite the higher $PM_{2.5}$ concentration in 2020 CSF. The decreases in As, Cr, Fe, Pb, and Ti were likely to be due to reductions in industrial activities and traffic [24,53]. Among the metals studied, Fe, Mn, and Cu were the most abundant elements in $PM_{2.5}$ in both study years. The levels of Co, Cd, Pb, and Ti increased during the SF period compared to pre-SF in 2018, while they decreased in 2020. The As and Cr (VI) concentrations in both years exceeded the NAAQS guideline values of 0.006 and 0.000025 μg/m^3, respectively. Therefore, As and Cr (VI) may be of significant health concern.

The PCA results (Table 3) for the $PM_{2.5}$ showed three factors that had a total variance of 76.812% in 2018 CSF. The variance of the first, second, and third factors were 32.517%, 23.387%, and 20.907%, respectively. Factor 1 showed high Pb, Cr, and Ti loadings and low Co and Cu loadings, which were linked to industry sources. Factor 2 was associated with combustion sources, with high loads of EC, OC, and Mn. Factor 3, contributing to the high loading of mineral elements (Fe and Cu), was characterized by mineral/road dust. Three factors were also identified in 2020. Compared to 2018, the proportion of combustion sources remained at the same level, while industry sources decreased by 5.871%, likely because of the CLDs. Therefore, the industry emissions were the major underlying reasons for the change in the chemical component of $PM_{2.5}$ in Taizhou, potentially leading to different health threats. Secondary sources could also contribute to the sources of $PM_{2.5}$, which constitute a difference in total variance.

Table 3. Factor loadings of $PM_{2.5}$ in Taizhou.

2018	Principle Components			2020	Principle Components		
	PC1	PC2	PC3		PC1	PC2	PC3
OC		0.529		OC		0.738	
EC		0.938		EC		0.611	
As			0.777	As		0.725	
Cd				Cd			−0.661
Co	0.643			Co			
Cr	0.851			Cr			0.744
Cu	0.543		0.667	Cu	0.928		
Fe			0.782	Fe	0.856		
Mn		0.599		Mn	0.934		
Pb	0.958			Pb		0.704	
Ti	0.817			Ti			0.596
Variance, %	32.517	23.387	20.907	Variance, %	30.175	23.457	15.036
Cumulative, %	32.517	55.905	76.812	Cumulative, %	30.175	53.632	68.669
Source	Industry	Combustion	Mineral/road dust		Mineral/road dust	Combustion	Industry

3.2. Comparison of Health Risks Associated with Metals in $PM_{2.5}$ in 2018 and 2020

Human health risks associated with $PM_{2.5}$-bound metals during the sampling period were calculated, as shown in Tables 4 and 5. The noncarcinogenic risk posed by As, Co, Mn, and Ti in 2018 and As and Mn in 2020 exceeded the acceptable level (HQ > 1), while indicating the existence of significant noncarcinogenic risk. The carcinogenic risk posed by As, Cr (VI), and Pb also exceeded the accepted precautionary limit (1×10^{-6}) in 2018 and 2020, indicating exposure to $PM_{2.5}$-bound metals posed potential carcinogenic risks

during CSF. Using the PCA-identified sources as the basis, the HQ of two selected metals (Mn and As) in $PM_{2.5}$ mass was the highest for $PM_{2.5}$ from mineral/road dust sources and combustion sources, while the CRs of Cr (VI) and As were the highest for $PM_{2.5}$ from industry sources.

Table 4. Noncarcinogenic risks via inhalation exposure to $PM_{2.5}$-bound metals during SF.

HQ	RfCi (mg/m^3)	2018		2020		
		Pre-SF	SF	Pre-SF	SF	Post-SF
As	1.5×10^{-5}	**2.77** ± 0.60	**2.77** ± 0.68	**2.30** ± 0.66	0.99 ± 0.78	**1.17** ± 0.86
Ba	5×10^{-4}	-	-	0.15 ± 0.01	0.26 ± 0.23	0.16 ± 0.02
Cd	1×10^{-5}	-	-	0.23 ± 0.07	0.14 ± 0.13	0.16 ± 0.06
Co	6×10^{-6}	**1.16** ± 0.21	**1.55** ± 0.12	-	-	-
Cr(VI)	1×10^{-4}	0.09 ± 0.02	0.11 ± 0.01	0.04 ± 0.00	0.05 ± 0.01	0.05 ± 0.00
Mn	5×10^{-5}	**4.99** ± 0.92	**2.95** ± 1.59	**4.13** ± 0.04	**5.35** ± 0.13	**4.36** ± 0.05
Ti	1×10^{-4}	0.76 ± 0.26	**1.12** ± 0.14	0.17 ± 0.01	0.17 ± 0.01	0.15 ± 0.02

Table 5. Carcinogenic risks via inhalation exposure to $PM_{2.5}$-bound metals during SF.

CR	IUR $(\mu g/m^3)^{-1}$	2018		2020		
		pre-SF	SF	pre-SF	SF	post-SF
As	4.3×10^{-3}	$\mathbf{6.12 \times 10^{-5}} \pm 1.32 \times 10^{-5}$	$\mathbf{6.12 \times 10^{-5}} \pm 1.50 \times 10^{-5}$	$\mathbf{5.09 \times 10^{-5}} \pm 1.45 \times 10^{-5}$	$\mathbf{2.18 \times 10^{-5}} \pm 1.73 \times 10^{-5}$	$\mathbf{2.59 \times 10^{-5}} \pm 1.91 \times 10^{-5}$
Cd	1.8×10^{-3}	-	-	$7.84 \times 10^{-9} \pm 2.42 \times 10^{-9}$	$4.79 \times 10^{-9} \pm 4.49 \times 10^{-9}$	$5.50 \times 10^{-9} \pm 2.11 \times 10^{-9}$
Co	9×10^{-3}	$1.43 \times 10^{-8} \pm 2.57 \times 10^{-9}$	$1.92 \times 10^{-8} \pm 1.46 \times 10^{-9}$	-	-	-
Cr(VI)	8.4×10^{-2}	$\mathbf{2.60 \times 10^{-4}} \pm 4.43 \times 10^{-5}$	$\mathbf{3.18 \times 10^{-4}} \pm 2.66 \times 10^{-5}$	$\mathbf{1.29 \times 10^{-4}} \pm 1.08 \times 10^{-5}$	$\mathbf{1.37 \times 10^{-4}} \pm 1.59 \times 10^{-5}$	$\mathbf{1.35 \times 10^{-4}} \pm 1.42 \times 10^{-5}$
Pb	8×10^{-5}	$\mathbf{2.38 \times 10^{-6}} \pm 9.20 \times 10^{-7}$	$\mathbf{4.23 \times 10^{-6}} \pm 1.62 \times 10^{-6}$	$\mathbf{1.18 \times 10^{-6}} \pm 2.73 \times 10^{-8}$	$9.34 \times 10^{-7} \pm 3.15 \times 10^{-8}$	$5.88 \times 10^{-7} \pm 2.44 \times 10^{-8}$

Among the evaluated metals, Mn, accounting for 34.68–51.10% and 58.83–76.99% of the total noncarcinogenic risk to humans in 2018 and 2020, respectively, and Cr (VI), accounting for approximately 80% of the total carcinogenic risk, were the major pollutants. Cr (VI) showed the largest CR in $PM_{2.5}$, implying its associated source, industry, was the greatest risk to people in Taizhou after exposure to $PM_{2.5}$.

Although the health risks of Fe and Cu are not discussed in this study, as their RfC_i values were not available, the presence of these metals in particles is still of concern, as transition metals were found to be associated with oxidative stress [54–58] and iron metabolism may be involved in the development of cancer [59].

4. Conclusions

This study examined the characteristics, sources, and health risks of metals associated with $PM_{2.5}$ during the CSF in Taizhou. $PM_{2.5}$ samples were collected in 2018 and 2020. The results showed a decreasing trend in both the mean and median $PM_{2.5}$ concentrations throughout the study period in 2018 and 2020. In addition, despite the lockdown measures, the average $PM_{2.5}$ concentration in 2020 was higher than in 2018, reaching three–four times the recommended annual value (35 $\mu g/m^3$) of China's National Ambient Air Quality Standard, which may be due to the synergistic effects of emissions, chemistry, and transport during CSF-2020. Compared to CSF-2018, the CM and elements were reduced by 39.41% and 53.84%, respectively, during CSF-2020, which should be attributed to the lockdown measures. The proportion of carbonaceous substances to $PM_{2.5}$ indicate a decrease in the relative contribution of primary emissions during the SF period and an increase in the

relative contribution of secondary emissions in the post-SF period. Fe, Mn, and Cu were the predominant metals. Of all carcinogenic metals, As and Cr(VI) exceeded the values set by the NAAQS guideline. PCA was applied to identify the possible carbonaceous and metal sources contributing to air pollution during the CSF. Combustion, industry, and soil sources were identified as the $PM_{2.5}$ sources and accounted for about 76% and 68% of the total variance in 2018 and 2020, respectively. The industry source was reduced by 5.87% with the impact of the city lockdown.

The health risk assessment showed that the total HQ and the total CR were higher than the acceptable limits during the CSF. The individual HQs for As, Co, and Mn and the individual CRs for As, Cr(VI), and Pb were above the acceptable limits in $PM_{2.5}$. Mn and Cr(VI) were the major pollutants. Industry sources were the largest risk to people after exposure to $PM_{2.5}$ in Taizhou.

This study has some limitations. For example, meteorological parameters were not measured at the sampling site. $PM_{2.5}$ sources could be better identified if water-soluble ions were included and more samples were taken. Nevertheless, the findings provide scientific evidence for understanding the air quality and, thus, public health in Taizhou during the CSF. Detailed exposure assessment for the specific sources of $PM_{2.5}$ based on health protection objectives can help make a considerable effort in air quality improvement. Control strategies and regional joint management efforts are important for the effective removal of air pollutants.

Supplementary Materials: The following supporting information can be downloaded at: https://www.mdpi.com/article/10.3390/atmos13122099/s1, Table S1: Pollutant concentrations (μg/m3) and meteorological conditions during the CSF.

Author Contributions: Conceptualization, S.H.; methodology, S.H. and Q.W.; software, K.J.; validation, K.J., H.Q., Q.W. and S.H.; formal analysis, Q.W.; investigation, Q.W., X.W. and W.F.; resources, S.H.; data curation, X.W.; writing—original draft preparation, Q.W. and X.W.; writing—review and editing, S.H.; visualization, W.F.; supervision, S.H. and D.W.; project administration, S.H., T.H. and J.L.; funding acquisition, S.H., T.H. and J.L. All authors have read and agreed to the published version of the manuscript.

Funding: This work received funding from the Postdoctoral Science Foundation of Jiangxi Province (no. 2016KY13), the Science and Technology Research Project of Jiangxi education department (no. 60011), Youth Science Foundation of Jiangxi Province (no. 20181BAB213017), and the National Natural Science Foundation of China (no. 52064037).

Institutional Review Board Statement: Not applicable.

Informed Consent Statement: Not applicable.

Data Availability Statement: The pollutant concentrations in Table S1 in supplementary file can be found at the China National Environmental Monitoring Center website http://www.cnemc.cn/. The meteorological data in Table S1 can be found at the China meteorological data network website http://data.cma.cn.

Acknowledgments: The authors are grateful for the above financial support and thank the two anonymous reviewers for their insightful comments.

Conflicts of Interest: The authors declare no conflict of interest.

References

1. Wang, H.; Gao, Z.; Ren, J.; Liu, Y.; Chang, L.T.-C.; Cheung, K.; Feng, Y.; Li, Y. An urban-rural and sex differences in cancer incidence and mortality and the relationship with PM2.5 exposure: An ecological study in the southeastern side of Hu line. *Chemosphere* **2019**, *216*, 766–773. [CrossRef] [PubMed]
2. Wu, C.; Wang, G.; Wang, J.; Li, J.; Ren, Y.; Zhang, L.; Cao, C.; Li, J.; Ge, S.; Xie, Y.; et al. Chemical characteristics of haze particles in Xi'an during Chinese Spring Festival: Impact of fireworks burning. *J. Environ. Sci.* **2018**, *71*, 179–187. [CrossRef] [PubMed]
3. Singh, A.; Pant, P.; Pope, F.D. Air quality during and after festivals: Aerosol concentrations, composition and health effects. *Atmos. Res.* **2019**, *227*, 220–232. [CrossRef]

4. Dai, L.; Zanobetti, A.; Koutrakis, P.; Schwartz, J.D. Associations of fine particulate matter species with mortality in the United States: A multicity time-series analysis. *Environ. Health Perspect.* **2014**, *122*, 837–842. [CrossRef]
5. Dehghani, M.; Keshtgar, L.; Javaheri, M.R.; Derakhshan, Z.; Conti, G.O.; Zuccarello, P.; Ferrante, M. The effects of air pollutants on the mortality rate of lung cancer and leukemia. *Mol. Med. Rep.* **2017**, *15*, 3390–3397. [CrossRef] [PubMed]
6. Lee, B.-J.; Kim, B.; Lee, K. Air pollution exposure and cardiovascular disease. *Toxicol. Res.* **2014**, *30*, 71–75. [CrossRef]
7. Zhang, Y.-L.; Cao, F. Fine particulate matter (PM2.5) in China at a city level. *Sci. Rep.* **2015**, *5*, 14884. [CrossRef] [PubMed]
8. Xie, J.; Jin, L.; Cui, J.; Luo, X.; Li, J.; Zhang, G.; Li, X. Health risk-oriented source apportionment of PM2.5-associated trace metals. *Environ. Pollut.* **2020**, *262*, 114655. [CrossRef] [PubMed]
9. Sørensen, M.; Schins, R.P.; Hertel, O.; Loft, S. Transition metals in personal samples of PM2.5 and oxidative stress in human volunteers. *Cancer Epidemiol. Biomark. Prev.* **2005**, *14*, 1340–1343. [CrossRef]
10. Liu, P.; Lei, Y.; Ren, H.; Gao, J.; Xu, H.; Shen, Z.; Zhang, Q.; Zheng, C.; Liu, H.; Zhang, R.; et al. Seasonal Variation and Health Risk Assessment of Heavy Metals in PM2.5 during Winter and Summer over Xi'an, China. *Atmosphere* **2017**, *8*, 91. [CrossRef]
11. Jiang, N.; Duan, S.; Yu, X.; Zhang, R.; Wang, K. Comparative major components and health risks of toxic elements and polycyclic aromatic hydrocarbons of PM2.5 in winter and summer in Zhengzhou: Based on three-year data. *Atmos. Res.* **2018**, *213*, 173–184. [CrossRef]
12. Liu, L.; Zhang, J.; Du, R.; Teng, X.; Hu, R.; Yuan, Q.; Tang, S.; Ren, C.; Huang, X.; Xu, L.; et al. Chemistry of Atmospheric Fine Particles During the COVID-19 Pandemic in a Megacity of Eastern China. *Geophys. Res. Lett.* **2021**, *48*, 2020GL091611. [CrossRef] [PubMed]
13. Karagulian, F.; Belis, C.A.; Dora, C.F.C.; Prüss-Ustün, A.M.; Bonjour, S.; Adair-Rohani, H.; Amann, M. Contributions to cities' ambient particulate matter (PM): A systematic review of local source contributions at global level. *Atmos. Environ.* **2015**, *120*, 475–483. [CrossRef]
14. Thurston, G.D.; Ito, K.; Lall, R. A source apportionment of U.S. fine particulate matter air pollution. *Atmos. Environ.* **2011**, *45*, 3924–3936. [CrossRef] [PubMed]
15. Cheng, N.; Zhang, C.; Jing, D.; Li, W.; Guo, T.; Wang, Q.; Li, S. An integrated chemical mass balance and source emission inventory model for the source apportionment of PM2.5 in typical coastal areas. *J. Environ. Sci.* **2020**, *92*, 118–128. [CrossRef]
16. Jiang, Q.; Sun, Y.L.; Wang, Z.; Yin, Y. Aerosol composition and sources during the Chinese Spring Festival: Fireworks, secondary aerosol, and holiday effects. *Atmos. Chem. Phys.* **2015**, *15*, 6023–6034. [CrossRef]
17. Feng, J.; Yu, H.; Su, X.; Liu, S.; Li, Y.; Pan, Y.; Sun, J.-H. Chemical composition and source apportionment of PM2.5 during Chinese Spring Festival at Xinxiang, a heavily polluted city in North China: Fireworks and health risks. *Atmos. Res.* **2016**, *182*, 176–188. [CrossRef]
18. Becker, J.M.; Iskandrian, S.; Conkling, J. Fatal and near-fatal asthma in children exposed to fireworks. *Ann. Allergy Asthma Immunol.* **2000**, *85*, 512–513. [CrossRef]
19. Liu, J.; Chen, Y.; Chao, S.; Cao, H.; Zhang, A. Levels and health risks of PM2.5-bound toxic metals from firework/firecracker burning during festival periods in response to management strategies. *Ecotoxicol. Environ. Saf.* **2019**, *171*, 406–413. [CrossRef] [PubMed]
20. Yang, L.; Gao, X.; Wang, X.; Nie, W.; Wang, J.; Gao, R.; Xu, P.; Shou, Y.; Zhang, Q.; Wang, W. Impacts of firecracker burning on aerosol chemical characteristics and human health risk levels during the Chinese New Year Celebration in Jinan, China. *Sci. Total Environ.* **2014**, *476*, 57–64. [CrossRef] [PubMed]
21. Pirker, L.; Velkavrh, Ž.; Osīte, A.; Drinovec, L.; Močnik, G.; Remškar, M. Fireworks—A source of nanoparticles, PM2.5, PM10, and carbonaceous aerosols. *Air Qual. Atmos. Health* **2022**, *15*, 1275–1286. [CrossRef]
22. Nasir, U.P.; Brahmaiah, D. Impact of fireworks on ambient air quality: A case study. *Int. J. Environ. Sci. Technol.* **2015**, *12*, 1379–1386. [CrossRef]
23. Huang, C.; Wang, Y.; Li, X.; Ren, L.; Zhao, J.; Hu, Y.; Zhang, L.; Fan, G.; Xu, J.; Gu, X.; et al. Clinical features of patients infected with 2019 novel coronavirus in Wuhan, China. *Lancet* **2020**, *395*, 497–506. [CrossRef] [PubMed]
24. Dai, Q.; Ding, J.; Song, C.; Liu, B.; Bi, X.; Wu, J.; Zhang, Y.; Feng, Y.; Hopke, P.K. Changes in source contributions to particle number concentrations after the COVID-19 outbreak: Insights from a dispersion normalized PMF. *Sci. Total Environ.* **2021**, *759*, 143548. [CrossRef]
25. Kraemer, M.U.; Yang, C.-H.; Gutierrez, B.; Wu, C.-H.; Klein, B.; Pigott, D.M.; Group†, O.C.-D.W.; Plessis, L.D.; Faria, N.R.; Li, R. The effect of human mobility and control measures on the COVID-19 epidemic in China. *Science* **2020**, *368*, 493–497. [CrossRef]
26. Tian, H.; Liu, Y.; Li, Y.; Wu, C.-H.; Chen, B.; Kraemer, M.U.; Li, B.; Cai, J.; Xu, B.; Yang, Q. An investigation of transmission control measures during the first 50 days of the COVID-19 epidemic in China. *Science* **2020**, *368*, 638–642. [CrossRef]
27. Rodríguez-Urrego, D.; Rodríguez-Urrego, L. Air quality during the COVID-19: PM2.5 analysis in the 50 most polluted capital cities in the world. *Environ. Pollut.* **2020**, *266*, 115042. [CrossRef] [PubMed]
28. Chauhan, A.; Singh, R.P. Decline in PM2.5 concentrations over major cities around the world associated with COVID-19. *Environ. Res.* **2020**, *187*, 109634. [CrossRef]
29. Chen, H.; Huo, J.; Fu, Q.; Duan, Y.; Xiao, H.; Chen, J. Impact of quarantine measures on chemical compositions of PM2.5 during the COVID-19 epidemic in Shanghai, China. *Sci. Total Environ.* **2020**, *743*, 140758. [CrossRef]
30. Tobías, A.; Carnerero, C.; Reche, C.; Massagué, J.; Via, M.; Minguillón, M.C.; Alastuey, A.; Querol, X. Changes in air quality during the lockdown in Barcelona (Spain) one month into the SARS-CoV-2 epidemic. *Sci. Total Environ.* **2020**, *726*, 138540. [CrossRef]

31. Le, T.; Wang, Y.; Liu, L.; Yang, J.; Yung, Y.L.; Li, G.; Seinfeld, J.H. Unexpected air pollution with marked emission reductions during the COVID-19 outbreak in China. *Science* **2020**, *369*, 702–706. [CrossRef] [PubMed]
32. Wang, H.; Miao, Q.; Shen, L.; Yang, Q.; Wu, Y.; Wei, H. Air pollutant variations in Suzhou during the 2019 novel coronavirus (COVID-19) lockdown of 2020: High time-resolution measurements of aerosol chemical compositions and source apportionment. *Environ. Pollut.* **2021**, *271*, 116298. [CrossRef] [PubMed]
33. Sulaymon, I.D.; Zhang, Y.; Hopke, P.K.; Hu, J.; Zhang, Y.; Li, L.; Mei, X.; Gong, K.; Shi, Z.; Zhao, B. Persistent high PM2.5 pollution driven by unfavorable meteorological conditions during the COVID-19 lockdown period in the Beijing-Tianjin-Hebei region, China. *Environ. Res.* **2021**, *198*, 111186. [CrossRef] [PubMed]
34. Chang, Y.; Huang, R.-J.; Ge, X.; Huang, X.; Hu, J.; Duan, Y.; Zou, Z.; Liu, X.; Lehmann, M.F. Puzzling Haze Events in China during the Coronavirus (COVID-19) Shutdown. *Geophys. Res. Lett.* **2020**, *47*, e2020GL088533. [CrossRef] [PubMed]
35. Kim, Y.; Jeon, K.; Park, J.; Shim, K.; Kim, S.-W.; Shin, H.-J.; Yi, S.-M.; Hopke, P.K. Local and transboundary impacts of PM2.5 sources identified in Seoul during the early stage of the COVID-19 outbreak. *Atmos. Pollut. Res.* **2022**, *13*, 101510. [CrossRef] [PubMed]
36. USEPA. *Risk Assessment Guidance for Superfund Volume I: Human Health Evaluation Manual (Part F, Supplemental Guidance for Inhalation Risk Assessment)*; EPA-540-R-070-002, OSWER 9285.7-82; Office of Superfund Remediation and Technology Innovation, United States Environmental Protection Agency: Washington, DC, USA, 2009; pp. 13–24.
37. USEPA. *Risk-Assessment Guidance for Superfund. Volume 1. Human Health Evaluation Manual. Part A. Interim Report (Final)*; EPA/540/1-89/002; Office of Solid Waste and Emergency Response: Washington, DC, USA, 1989; pp. 8–28.
38. USEPA. *Risk Assessment Guidance for Superfund, Volume 1, Human Health Evaluation Manual (Part B, Development of Risk-Based Preliminary Remediation Goals)*; EPA/540/R-92/003; Office of Emergencyand Remedical Response: Washington, DC, USA, 1991; pp. 1–4.
39. USEPA. *Regional Screening Level (RSL) Summary Table (TR = 1E-06, HQ = 1)*; US Environmental Protection Agency (EPA): Washington, DC, USA, 2021.
40. Taner, S.; Pekey, B.; Pekey, H. Fine particulate matter in the indoor air of barbeque restaurants: Elemental compositions, sources and health risks. *Sci. Total Environ.* **2013**, *454–455*, 79–87. [CrossRef] [PubMed]
41. Xue, W.; Shi, X.; Yan, G.; Wang, J.; Xu, Y.; Tang, Q.; Wang, Y.; Zheng, Y.; Lei, Y. Impacts of meteorology and emission variations on the heavy air pollution episode in North China around the 2020 Spring Festival. *Sci. China Earth Sci.* **2021**, *64*, 329–339. [CrossRef] [PubMed]
42. Xu, H.; Chen, L.; Chen, J.; Bao, Z.; Wang, C.; Gao, X.; Cen, K. Unexpected rise of atmospheric secondary aerosols from biomass burning during the COVID-19 lockdown period in Hangzhou, China. *Atmos. Environ.* **2022**, *278*, 119076. [CrossRef]
43. An, Z.; Huang, R.-J.; Zhang, R.; Tie, X.; Li, G.; Cao, J.; Zhou, W.; Shi, Z.; Han, Y.; Gu, Z.; et al. Severe haze in northern China: A synergy of anthropogenic emissions and atmospheric processes. *Proc. Natl. Acad. Sci. USA* **2019**, *116*, 8657–8666. [CrossRef]
44. Guo, S.; Hu, M.; Zamora, M.L.; Peng, J.; Shang, D.; Zheng, J.; Du, Z.; Wu, Z.; Shao, M.; Zeng, L.; et al. Elucidating severe urban haze formation in China. *Proc. Natl. Acad. Sci. USA* **2014**, *111*, 17373–17378. [CrossRef] [PubMed]
45. Wang, Y.; Yuan, Y.; Wang, Q.; Liu, C.; Zhi, Q.; Cao, J. Changes in air quality related to the control of coronavirus in China: Implications for traffic and industrial emissions. *Sci. Total Environ.* **2020**, *731*, 139133. [CrossRef]
46. Luo, K.; Wang, Z.; Wu, J. Association of population migration with air quality: Role of city attributes in China during COVID-19 pandemic (2019–2021). *Atmos. Pollut. Res.* **2022**, *13*, 101419. [CrossRef] [PubMed]
47. Wang, S.; Yu, R.; Shen, H.; Wang, S.; Hu, Q.; Cui, J.; Yan, Y.; Huang, H.; Hu, G. Chemical characteristics, sources, and formation mechanisms of PM2.5 before and during the Spring Festival in a coastal city in Southeast China. *Environ. Pollut.* **2019**, *251*, 442–452. [CrossRef]
48. Feng, J.; Sun, P.; Hu, X.; Zhao, W.; Wu, M.; Fu, J. The chemical composition and sources of PM2.5 during the 2009 Chinese New Year's holiday in Shanghai. *Atmos. Res.* **2012**, *118*, 435–444. [CrossRef]
49. Wu, K.; Duan, M.; Liu, H.; Zhou, Z.; Deng, Y.; Song, D.; Tan, Q. Characterizing the composition and evolution of firework-related components in air aerosols during the Spring Festival. *Environ. Geochem. Health* **2018**, *40*, 2761–2771. [CrossRef] [PubMed]
50. Turpin, B.J.; Huntzicker, J.J. Identification of secondary organic aerosol episodes and quantitation of primary and secondary organic aerosol concentrations during SCAQS. *Atmos. Environ.* **1995**, *29*, 3527–3544. [CrossRef]
51. Zhang, J.; Liu, L.; Wang, Y.; Ren, Y.; Wang, X.; Shi, Z.; Zhang, D.; Che, H.; Zhao, H.; Liu, Y.; et al. Chemical composition, source, and process of urban aerosols during winter haze formation in Northeast China. *Environ. Pollut.* **2017**, *231*, 357–366. [CrossRef] [PubMed]
52. Wang, P.; Chen, K.; Zhu, S.; Wang, P.; Zhang, H. Severe air pollution events not avoided by reduced anthropogenic activities during COVID-19 outbreak, Resources. *Conserv. Recycl.* **2020**, *158*, 104814. [CrossRef] [PubMed]
53. Hong, Y.; Xu, X.; Liao, D.; Zheng, R.; Ji, X.; Chen, Y.; Xu, L.; Li, M.; Wang, H.; Xiao, H.; et al. Source apportionment of PM2.5 and sulfate formation during the COVID-19 lockdown in a coastal city of southeast China. *Environ. Pollut.* **2021**, *286*, 117577. [CrossRef]
54. Nieuwenhuijsen, M.J.; Gómez-Perales, J.E.; Colvile, R.N. Levels of particulate air pollution, its elemental composition, determinants and health effects in metro systems. *Atmos. Environ.* **2007**, *41*, 7995–8006. [CrossRef]
55. Winterbourn, C.C. Toxicity of iron and hydrogen peroxide the Fenton reaction. *Toxicol. Lett.* **1995**, *82–83*, 969–974. [CrossRef] [PubMed]

56. Park, J.; Park, E.H.; Schauer, J.J.; Yi, S.-M.; Heo, J. Reactive oxygen species (ROS) activity of ambient fine particles (PM2.5) measured in Seoul, Korea. *Environ. Int.* **2018**, *117*, 276–283. [PubMed]
57. Keeling, B.; Li, K.Y.; Churg, A. Iron enhances uptake of mineral particles and increases lipid peroxidation in tracheal epithelial cells. *Am. J. Respir. Cell Mol. Biol.* **1994**, *10*, 683–688. [CrossRef] [PubMed]
58. Chen, S.; Li, D.; Wu, X.; Chen, L.; Zhang, B.; Tan, Y.; Yu, D.; Niu, Y.; Duan, H.; Li, Q.; et al. Application of cell-based biological bioassays for health risk assessment of PM2.5 exposure in three megacities, China. *Environ. Int.* **2020**, *139*, 105703. [CrossRef]
59. Park, E.J.; Kim, S.N.; Lee, G.H.; Jo, Y.M.; Yoon, C.; Kim, D.W.; Cho, J.W.; Han, J.S.; Lee, S.J.; Seong, E.; et al. Inhaled underground subway dusts may stimulate multiple pathways of cell death signals and disrupt immune balance. *Environ. Res.* **2020**, *191*, 109839. [CrossRef]